Misfit-layered compound $PbTiS_3$ with incommensurate modulation: Transmission electron microscopy analysis and transport properties*

Shen Xi(沈 希)[a], Cheng Dan(程 丹)[b], Zhao Hao-Fei(赵豪飞)[a],
Yao Yuan(姚 湲)[a], Liu Xiao-Yang(刘晓旸)[b], and Yu Ri-Cheng(禹日成)[a]†

[a] *Beijing National Laboratory for Condensed Matter Physics, Institute of Physics, Chinese Academy of Sciences, Beijing* 100190, *China*
[b] *State Key Laboratory of Inorganic Synthesis and Preparative Chemistry, Jilin University, Changchun* 130021, *China*

(Received 24 May 2013; revised manuscript received 27 July 2013)

The microstructural characteristic of the misfit-layered compound $PbTiS_3$ has been studied with transmission electron microscopy. All the incommensurate modulation-induced satellite spots and main diffraction spots of basic sublattices can be indexed systematically with a superspace group method. Finally, the relationship between the electronic transport properties and the crystal structure is discussed.

Keywords: incommensurate modulation, misfit-layered sulfide, transmission electron microscopy

PACS: 61.44.Fw, 68.37.Lp, 68.37.Og, 61.05.J– **DOI:** 10.1088/1674-1056/22/11/116102

1. Introduction

In the last four decades, much attention has been paid to the misfit-layered compounds with a general formula $(MX)_x(TX_2)_y$, where X is usually O, S, or Se; M is a divalent cation such as Pb or Sr; T is a transition metal element such as Nb, Cr, Ti, or V; $x = 1.12$–2; and $y = 1$–2, because of their unique crystal structures.[1–6] These compounds can be classified as an incommensurate crystal system characterized by two sublattices MX and TX_2 that have an alternate stacking arrangement and contain the same periodicity of lattice along the c axis. Furthermore, the MX sublattice with a distorted rock salt structure can be regarded as an intercalation layer into a van der Waals gap between the TX_2 double sublattices where the transition metal cation occupies the center of an octahedron comprising six chalcogen atoms. Since the two types of sublattices possess an irrational ratio of lattice constant along one direction and common periodicity in the other direction in the ab plane,[2,6–10] a strain induced by the misfit between MX and TX_2 sublattices may cause a peculiar one-dimensional incommensurate modulation which is nearly perpendicular to the c axis.

Although the superconducting, magnetic, and electric properties of misfit-layered compounds were reported a long time ago,[11–14] more interest has been concentrated on the intercalation intergrowth combining misfit-layered compounds with metal cations as guest materials due to their widespread and successful applications, such as lithium batteries and sensors.[3,5,9,15,16] Thus, a lot of misfit-layered compounds have been used as host materials in order to enhance the charge transfer from guest to host. As a desired candidate material, a Pb–Ti–S system consists of two real compositions: $(PbS)_{1.18}(TiS_2)$ and $(PbS)_{1.18}(TiS_2)_2$, both of which are determined to have a monoclinic structure.[17,18] The structure of the former compound (nominal composition $PbTiS_3$) can be described in terms of an alternate stacking of monoclinic PbS and TiS_2 sublattices along the c axis and a mutual incommensurate modulation along the a axis. Besides, Smaalen *et al.*[6] reported that a polytype of structure in $(PbS)_{1.18}(TiS_2)$ comprises the monoclinic unit cell and its mirror image, which forms a new orthorhombic crystal symmetry with about a double c parameter.

In this paper, we focus on the microstructural investigation of misfit-layered compound $PbTiS_3$ by transmission electron microscopy (TEM), which is valuable for studying superstructures of compounds.[19] In particular, we report the observation of an incommensurately modulated structure along the misfit direction between sublattices. Moreover, the transport properties of this layered sample, both parallel and perpendicular to the ab plane, which can be associated with the structural characteristics, are also discussed.

2. Experiment

The misfit-layered compound $PbTiS_3$ was synthesized as a high quality single crystal that shows an ultrathin slice morphology with several-millimeter dimensions along its ab plane. The detailed synthesis procedures were described in a previous work.[20] $PbTiS_3$ crystals were prepared by direct reaction of lead powder, titanium powder, and sulfur sublimate in quartz tubes with a diameter of 11 mm and a length of 120 mm. The powders were ground with a molar ratio of

*Project supported by the National Basic Research Program of China (Grant No. 2012CB932302), the National Natural Science Foundation of China (Grant No. 50921091), and the Specific Funding of the Discipline and Graduate Education Project of Beijing Municipal Commission of Education, China.

†Corresponding author. E-mail: rcyu@aphy.iphy.ac.cn

© 2013 Chinese Physical Society and IOP Publishing Ltd

Pb:Ti:S = 1:1:3.5 of the reactants. The reactant mixture was transferred into tubes that were closed at one end. The loaded tubes were evacuated (1.33×10^{-2} Pa), sealed, and heated in a horizontal-tube furnace. Then a mass of grey-black plate-like samples, up to 15 mm×10 mm×0.01 mm in size, were obtained on the inner surfaces of the tubes at the cool end after they had been heated at 973 K for 6 days. The TEM plane specimen was prepared by argon ion beam polishing perpendicular to the c axis of the compound. Moreover, for the cross-section specimen, the compound was sandwiched between a couple of silicon pieces and polished by an argon ion beam parallel to the c axis after mechanical thinning. A liquid nitrogen cold stage, low voltage, and a small angle of ionic guns were applied during ion polishing to reduce the damage from the ion beams. Philips CM200 and FEI Tecnai F20 transmission electron microscopes (TEMs) with a field emission gun operated at 200 keV were used for select-area electron diffraction (SAED), bright-field (BF) TEM, and high-resolution TEM (HRTEM) investigations. The measurements for the electrical transport properties parallel and perpendicular to the ab planes of the single crystal samples were carried out on a Mag Lab system (Oxford instruments) using the standard four-probe technique.

3. Results and discussion

3.1. TEM analysis of the misfit-layered compound $PbTiS_3$

In the last decade, though similar compounds were studied by TEM,[21–23] very detailed studies on the $PbTiS_3$ compound by TEM are not sufficient. In order to confirm the crystal structure of this compound, the TEM observations were performed, and BF TEM images of the plane and cross-section specimens are shown in Figs. 1(a) and 1(b), respectively. It is obvious that the microstructure of the cross-section specimen has a spread of alternating dark and bright stripes across the whole region in Fig. 1(b) due to misorientation among the ab plane.

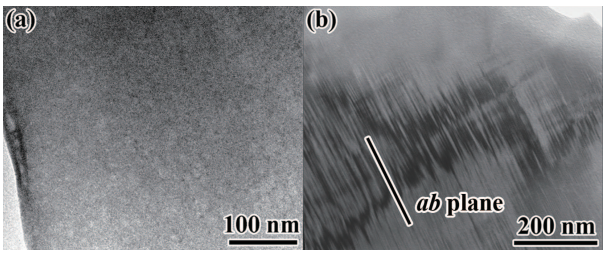


Fig. 1. BF TEM images of the (a) plane and (b) cross-section specimens of the $PbTiS_3$ compound at low magnification.

Figure 2 is a modulated crystal structure of the misfit-layered compound $PbTiS_3$, which is illustrated according to the refined coordinate's parameters obtained from single crystal X-ray diffraction by Smaalen *et al.*[17] The structure is built up on the basis of a superspace with two mutually incommensurate monoclinic sublattices stacking alternately along the c axis. This is the corresponding method used to describe the special modulated structure of quasicrystals.[24] The first sublattice (I) is formed by the distorted NaCl-type PbS double layer with lattice constants $a_{\rm I} = 0.5800$ nm, $b_{\rm I} = 0.5881$ nm, $c_{\rm I} = 1.1759$ nm, $\beta_{\rm I} = 95.27^\circ$ and space group $C2/m$. In the second sublattice (II) (the TiS_2 layer) with lattice constants $a_{\rm II} = 0.3409$ nm, $b_{\rm II} = 0.5880$ nm, $c_{\rm II} = 1.1760$ nm, $\beta_{\rm II} = 95.29^\circ$ and space group $C2_1/m$, each titanic atom is surrounded by six sulfur atoms composing an octahedron. In the report of Smaalen *et al.*,[17] the superspace is described with the average values of lattice constants of two sublattices ($b = 1/2(b_{\rm I} + b_{\rm II})$, $c = 1/2(c_{\rm I} + c_{\rm II})$, $\beta = 1/2(\beta_{\rm I} + \beta_{\rm II})$), except for $a = a_{\rm I}$ ($a_{\rm I} > a_{\rm II}$).

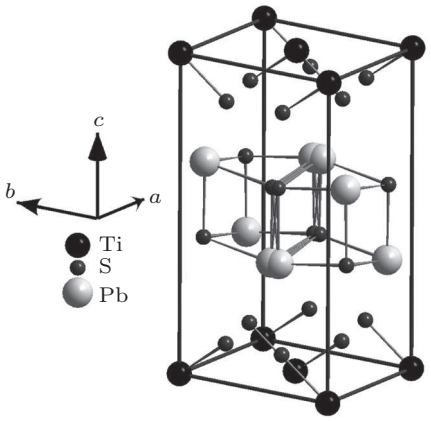


Fig. 2. Schematic model of the misfit-layered compound $PbTiS_3$ in one super cell. The small balls represent S atoms, the large light gray balls denote Pb atoms, and the large black balls indicate Ti atoms occupying the centers of octahedra.

In 2003, Brandt *et al.*[21] reported satellite spots around the main reflections in the compound $(PbS)_{1.18}TiS_2$ and deduced that these satellites originate from double reflections from both sublattices. However, in order to further obtain the microstructural information of our compound with TEM, a superspace group analysis was utilized with four basic translation vectors $\boldsymbol{M}^* = \{\boldsymbol{a}^*, \boldsymbol{b}^*, \boldsymbol{c}^*, \boldsymbol{q}\}$ (the $\boldsymbol{q}$ is defined as a modulated vector) in a (3 + 1)-dimensional reciprocal space.[2,7,17,25] Figures 3(a) and 3(b) show a typical SAED pattern and the corresponding HRTEM image along the [001] zone-axis direction, respectively. All the main reflections of the two sublattices can be indexed with integers (hkl) in Fig. 3(a). The rectangular dashed lines and the crosses indicate their unit cells and positions of extinction spots in the reciprocal space, respectively. According to the length ratio of lattice constant a calculated from the interplanar distances of $(200)_{\rm I}$ and $(200)_{\rm II}$, we can gain an irrational $x = 2a_{\rm II}/a_{\rm I} \sim 1.20$,[4,6,17,26] which defines the incommensurability, crystal structure, and accurate formula of $(MX)_x(TX_2)_y$ type misfit-layered compounds, in consistent with the results

of X-ray refinement.[17] Besides, we notice the occurrence of weak satellite spots, which are due to the misfit between PbS and TiS_2 sublattices along the $\boldsymbol{a}^*$ axis. Therefore, both the corresponding incommensurate modulation and the basic sublattice reflections are indexed systematically with integers $(hklm)$ considering the set of superspace groups, which are marked by the white arrows in Fig. 3(a). If the main spots of the TiS_2 sublattice are regarded as the satellite spots of the PbS sublattice, the basic reciprocal lattice vector for the superspace is $\boldsymbol{M}^* = h\boldsymbol{a}^* + k\boldsymbol{b}^* + l\boldsymbol{c}^* + \boldsymbol{q}$, where $\boldsymbol{a}^* = \boldsymbol{a}_{\rm I}^*$, $\boldsymbol{b}^* = 1/2(\boldsymbol{b}_{\rm I}^* + \boldsymbol{b}_{\rm II}^*)$, $\boldsymbol{c}^* = 1/2(\boldsymbol{c}_{\rm I}^* + \boldsymbol{c}_{\rm II}^*)$, and $\boldsymbol{q} = m\boldsymbol{a}_{\rm II}^*$, vice versa. In addition, all the reflection conditions can be concluded as: $h+k+m$ = odd gives rise to systematic extinction in the $(hklm)$ lattice planes in Fig. 3(a), which implies a C-centered symmetry operator. According to the results of Smaalen *et al.*,[17] the superspace group can be deduced as a monoclinic group $C2/m$ in three dimensions. Here, we also point out that the incident electron beam deviates from the c axis ([001] direction) slightly because of the existence of a small angle between the normal of the sublattice layers and the direction of the stacking axis.

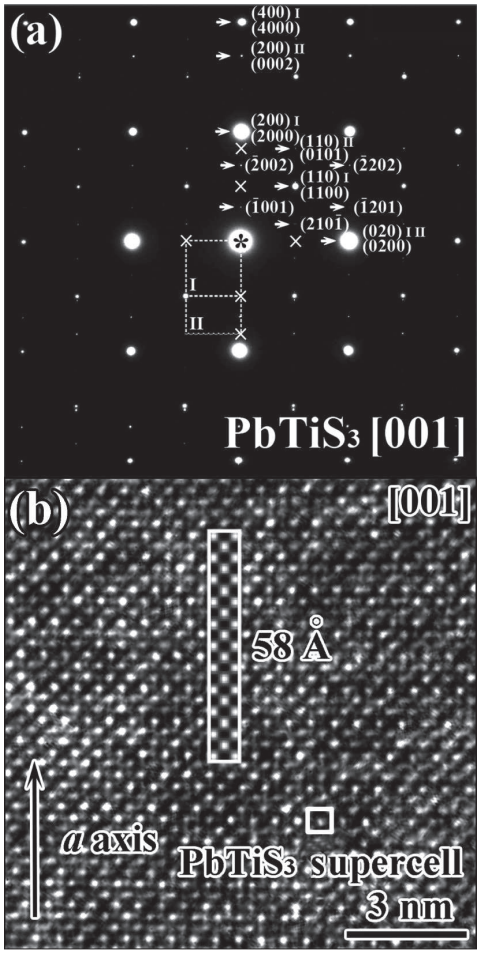


Fig. 3. (a) Typical SAED pattern and (b) the corresponding HRTEM image of the plane specimen along the [001] zone axis. In panel (a), the unit cells and positions of extinction spots are marked by the rectangular dashed lines and the crosses, respectively. In panel (b), the superspace cell is indicated by a white frame.

In Fig. 3(b), the superspace cell is indicated by a white frame in the *ab* plane. This image was obtained from a thin region of the crystal under the Scherzer focus. In addition, a simulated image for a crystal thickness of 25.9 nm and a defocus value of −76 nm, superimposed onto the image, fits perfectly with the experimental result on the basis of the misfit-layered structure.[17] Although the ratio of the sublattice constants is irrational along the a axis, we may gain a repetition period of 5.8 nm approximately, which corresponds to another long-range order of $10|\boldsymbol{a}_{\rm I}^*| \approx 17|\boldsymbol{a}_{\rm II}^*| \approx 5.8$ nm.

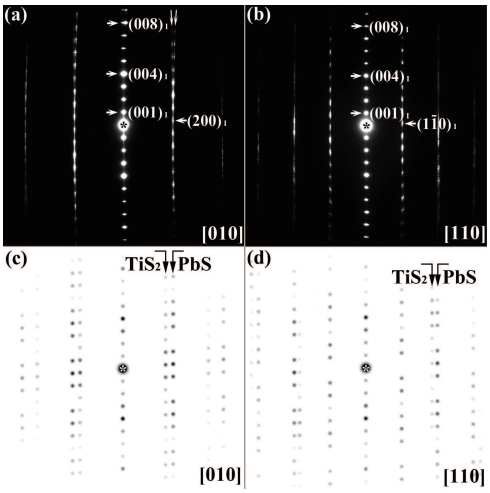


Fig. 4. (a), (b) SAED patterns recorded along [010] and [110] zone axes and (c), (d) their simulated patterns.

In major regions of the $PbTiS_3$ plane specimen, the [001] zone shown in Fig. 3 is observed frequently due to the high preferential orientation of a single crystal. Therefore, the microstructural information perpendicular to the c axis could only be obtained from the cross-section specimen of the $PbTiS_3$ compound. Figure 4 illustrates the SAED patterns recorded along the [010] and [110] zone axes and their simulated patterns. In order to simulate the incommensurately modulated structure, we constructed a superlattice with a repetition period of approximately 5.8 nm. It should be noted that there is a discrepancy between the selected superlattice structure and the real modulated structure. From the simulated SAED patterns shown in Figs. 4(c) and 4(d), one can observe the "additional" diffraction spots from the TiS_2 sublattice besides the diffraction spots of the PbS sublattice. However, in the experimental SAED patterns shown in Figs. 4(a) and 4(b), no additional diffraction spots are observed. On one hand, it could be caused by a discrepancy between the selected superlattice structure model and the real structure; on the other hand, in Fig. 3(a), the intensity of the $(200)_{\rm I}$ diffraction spot of the PbS sublattice is much higher than that of the $(200)_{\rm II}$ diffraction spot of the TiS_2 sublattice. Therefore, it is reasonable that the additional diffraction spots that belong to the TiS_2 sublattice are hardly detected in the exper-

iments as shown in Figs. 4(a) and 4(b). Elongated diffraction spots in the (*hk*0) series of lattice planes reveal the ultrathin layered characteristic of the compound. Meanwhile, we notice that the separation of some spots occurs, as marked by the white arrows in Fig. 4(a), indicating the existence of misorientation of the crystallites, which is observed usually in the cross-section specimen (Fig. 1(b)). The corresponding HRTEM images along [010] and [110] zone axes are shown in Figs. 5(a) and 5(b), respectively, which are similar to the results of Brandt *et al.*[21]

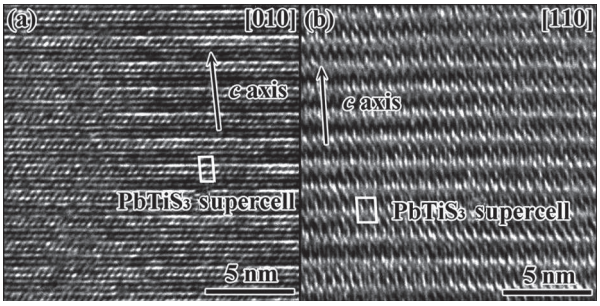


Fig. 5. HRTEM images along (a) [010] and (b) [110] zone axes from the cross-section specimen of $PbTiS_3$.

3.2. Transport properties of the misfit-layered compound $PbTiS_3$

The temperature dependencies of the resistivity of $PbTiS_3$ along the *ab* plane and the *c* axis are shown in Fig. 6. Both of them exhibit metallic characteristics despite the huge anisotropy in electrical conductivity, similar to those reported by Titov *et al.*[27] It is obvious that the resistivity parallel to the sublattice layers is smaller by about 10^4 orders of magnitude than that along the perpendicular direction. According to the theories of Ohno and Hangyo *et al.*,[8,10] when the PbS sublattice as a guest layer is intercalated into the host double TiS_2 sublattice layers, a weak interlayer interaction with low conductivity may be induced. As a result, every sublattice is weakly connected with its adjacent one along the stacking axis direction, suppressing the interlayer transfer of charge carriers along the *c* axis. Still, we may observe charge transfer between guest and host layers due to the difference of chemical potentials and Fermi levels, retaining the metallic properties of the sample along the *c* axis.

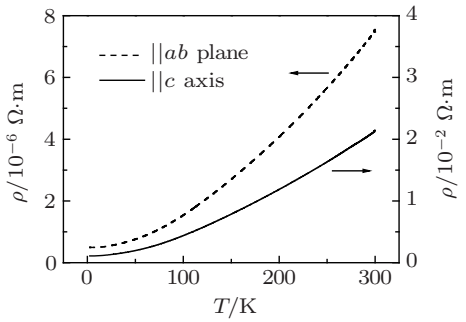


Fig. 6. Resistivity ρ versus temperature along the *ab* plane and the *c* axis of $PbTiS_3$.

4. Conclusion

The microstructure of misfit-layered compound $PbTiS_3$ has been analyzed with transmission electron microscopy. With a superspace group method, we have obtained the basic reciprocal lattice vector for the superspace cell and all the reflection conditions. The conductivity parallel to the sublattice layers is larger than that along the perpendicular direction.

References

[1] Garbrecht M, Spiecker E, Tillmann K and Jäger W 2011 *Ultramicroscopy* **111** 245
[2] Castillo-Martínez E, Schönleber A, van Smaalen S, Arévalo-López A M and Alario-Franco M A 2008 *J. Solid State Chem.* **181** 1840
[3] Hernán L, Morales J, Sánchez L, Tirado J L, Espinós J P and González Elipe A R 1995 *Chem. Mater.* **7** 1576
[4] Sourisseau C, Cavagnat R, Fouassier M, Tirado J L and Morales J 1995 *J. Mol. Struct.* **348** 107
[5] Hernán L, Morales J, Sánchez L and Tirado J L 1993 *Chem. Mater.* **5** 1167
[6] van Smaalen S and de Boer J L 1992 *Phys. Rev. B* **46** 2750
[7] Isobe M, Onode M, Shizuya M, Tanaka M and Takayama-Muromachi E 2007 *Philos. Mag.* **87** 2647
[8] Hangyo M, Nakashima S, Hamada Y and Nishio T 1993 *Phys. Rev. B* **48** 11291
[9] Barriga C, lavela P, Morales J, Pattanayak J and Tirado J L 1992 *Chem. Mater.* **4** 1021
[10] Ohno Y 1991 *Phys. Rev. B* **44** 1281
[11] Murugesan T, Ramesh S, Gopalakrishnan J and Rao C N R 1981 *J. Solid State Chem.* **38** 165
[12] Sterzel W and Horn J 1970 *Z. Anorg. Allg. Chem.* **376** 254
[13] Schmidt L 1970 *Phys. Lett.* **31A** 551
[14] Schmidt L, McCarthy S L and Maita J P 1970 *Solid State Commun.* **8** 1513
[15] Sidorov M, McKelvy M, Sharma R, Glaunsinger W, Ganal P, Moreau P and Ouvrard G 1995 *Chem. Mater.* **7** 1140
[16] Guzmán R, Hernán L, Morales J, Pattanayak J and Tirado J L 1993 *Mat. Res. Bull.* **28** 469
[17] van Smaalen S, Meetsma A, Wiegers G A and de Boer J L 1991 *Acta Cryst. B* **47** 314
[18] Meerschaut A, Auriel C and Rouxel J 1992 *J. Alloys Compd.* **183** 129
[19] Ge B H, Li F H, Li X M, Wang Y M, Chi Z H and Jin C Q 2008 *Chin. Phys. B* **17** 3163
[20] Cheng D, Jin H, Li B X, Wang X F, Chu Q X, Lv Y, Liu X Y and Zhao X D 2012 *Chem. Res. Chin. Univ.* **28** 171
[21] Brandt J, Kipp L, Skibowski M, Krasovskii E E, Schattke W, Spiecker E, Dieker C and Jäger W 2003 *Surf. Sci.* **532–535** 705
[22] van Smaalen S 2007 *Incommensurate crystallography* (London: Oxford University Press) pp. 11–26
[23] Gotoh Y, Goto M, Kawaguchi K, Oosawa Y and Onoda M 1990 *Mater. Res. Bull.* **25** 307
[24] Xu L and Mai Z H 1998 *Chin. Phys. Lett.* **15** 665
[25] Onoda M, Kato K, Gotoh Y and Oosawa Y 1990 *Acta Cryst. B* **46** 487
[26] Salamanca Oviedo L N, Gómez-Herrero A, Landa Cánovas A R and Otero-Díaz L C 2000 *Micron* **31** 597
[27] Titov A N, Shchennikov V V, Kar'kin A E and Titova S G 2000 *Phys. Solid State* **42** 422